Fluorescence Redox Switching Systems Operating through Metal Centres: the Ni^{III}/Ni^{II} Couple

Giancarlo De Santis, Luigi Fabbrizzi,* Maurizio Licchelli, Nicola Sardone and Aldo Hendrikus Velders

Abstract: The covalently linked two-component systems **3** and **4** display fluorescence redox switching activity: the Ni^{III} form quenches the fluorescence of the proximate aromatic fluorophore, whereas the Ni^{II} form does not. Thus, fluorescence can be switched on and off at will through the reversible Ni^{II}/Ni^{III} redox reaction, which is carried out both electrochemically (in MeCN) and chemically (in EtOH). Quenching of the excited fluorophore F* is ascribed to a thermodynamically favoured F*-to-Ni^{III} electron transfer mechanism. The more flexible system **5** does not work as a switch, since the fluorescence of the anthracene subunit is quenched in both Ni^{II} and Ni^{III} forms (an OFF/OFF situation), through an energy transfer mechanism. The crystal and molecular structure of **4** in its protonated form is also described.

Keywords
electron-transfer reactions · fluorescence · molecular devices · redox switches · nickel complexes

Introduction

The generation and treatment of signals at a molecular level is a novel branch of science (semiochemistry) at the crossroads of chemistry, physics and biology.[1] The design and engineering of molecular devices for signal generation and processing falls within the realms of supramolecular chemistry and requires the topologically correct assembly of several components possessing some specific features. A typical device should consist of an *active* unit (A) displaying an easily observable property (the signal) and a *control* unit (C), that is, a molecular fragment capable of existing in two different states of comparable stability (a *bistable* system).[2] The C unit should possess the following properties: 1) the reversible access to each state should be controlled from the outside through the variation of an environmental parameter (e.g., pH or a redox potential, if the device is to work in solution); 2) each state should modify the property of the A unit to a different extent. Once these conditions are fulfilled, a fine change in the environmental parameter should induce, through the C unit, a substantial change in the property of A, which will be perceived by the environment or an external observer as a signal. If the quantity expressing the property changes by two orders of magnitude or more, the property appears to be switched on and off, and the two-component systems can then be designated as *switching* devices (more precisely, the switch is the control unit). The active unit and the control unit can be connected covalently or noncovalently. In the simplest covalently linked C–A systems, a $-(CH_2)_n-$ bridge may suffice to keep the two subunits together. However, the features of the spacer are not irrelevant, as they affect the signal transduction mechanism and, ultimately, determine signalling efficiency.

Among switchable properties, fluorescence is perhaps the most convenient, as it can be unambiguously detected even at very low concentrations and can be switched on and off (restored/quenched) through well-defined mechanisms, namely, electron transfer (eT) and energy transfer (ET).[3] In particular, the occurrence/nonoccurrence of the eT process (which corresponds to the OFF/ON switching of fluorescence) is strictly related to the redox state of the control unit. Thus, redox interconversion between the two states may lead to fluorescence switching in a two-component system C–A* (Fig. 1). In particular, switching is obtained when one form of the C unit, either C_{ox} or C_{red}, induces an eT process to or from the photoexcited A* unit, whereas the other has no effect. Such a favourable condition is thermodynamically determined, and knowledge of the relevant thermodynamic quantities may allow the design of an assembly containing the appropriate C and A units to produce a luminescent switching device.

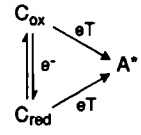

Fig. 1. The basis of redox switching activity in a covalently linked two-component system C–A.

The first system for redox switching of fluorescence, **1**, was reported by Lehn et al.[4] The control unit was a quinone/hydroquinone fragment, which was linked to the $[Ru^{II}(bpy)_3]^{2+}$ luminescent fragment. The quinone subunit (RO_2) is the C_{ox} form

[*] Prof. Dr. L. Fabbrizzi, Dr. M. Licchelli
Dipartimento di Chimica Generale, Università di Pavia
Via Taramelli 12, I-27100 Pavia (Italy)
Fax: Int. code +(382)528-544
e-mail: labfab@ipv85.unipv.it
Dr. G. De Santis
Dipartimento di Scienze, Università G. d'Annunzio
I-65127 Pescara (Italy)
Dr. N. Sardone
Centro Grandi Strumenti, Università di Pavia
Cascina Cravino, I-27100 Pavia (Italy)
A. H. Velders
Leiden Institute of Chemistry, Gorlaeus Laboratoria, Leiden University
2300 RA Leiden (The Netherlands)

  0947-6539/96/0210-1243 $ 15.00+.25/0

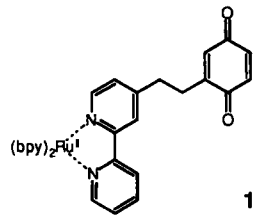

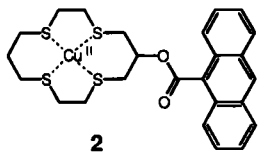

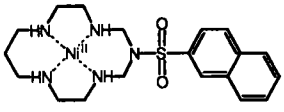

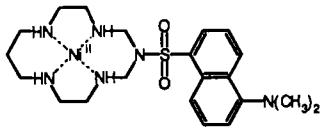

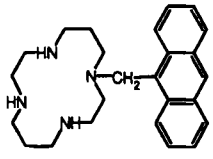

and induces an eT process from the adjacent light-emitting fragment, which causes luminescence quenching. On the other hand, the C_{red} form (hydroquinone, $R(OH)_2$) does not promote any eT process to the excited fluorophore. Thus, the fluorescence can be switched on and off through consecutive reduction and oxidation processes, which can be carried out both chemically and electrochemically in an aqueous solution. It should be noted that system **1**, whose C_{ox} and C_{red} states are separated by two electrons (and two protons: $RO_2 + 2e^- + 2H^+ \rightarrow R(OH)_2$), does not fit exactly the triangular scheme of Figure 1, in which the edges all involve one-electron processes. We have recently reported a further fluorescence switching device, **2**, based on a metal-centred one-electron redox couple (Cu^{II}/Cu^{I} inside a tetrathia macrocycle).[5] Again, the fluorescence of this system, which arises from a charge-transfer excited state of the 9-anthracenecarboxylic ester fragment, is quenched in the oxidised form C_{ox}–A*, through an A*-to-C_{ox} eT mechanism. As the C_{red}-to-A* eT process does not take place, reduction of Cu^{II} to Cu^{I} restores fluorescence, so that light emission can be consecutively switched on and off at will, by simply adjusting the potential of the working platinum electrode in an electrolysis experiment in acetonitrile solution. In the case of device **2**, the homogeneity of the redox and photoredox processes, which are all of the one-electron type, made it possible to account for the occurrence/nonoccurrence of the fluorescence quenching in terms of thermodynamics.

In order to examine the generality of the principles underlying the design of metal-centred redox switching devices, we move now to a different couple. In particular, we consider the Ni^{III}/Ni^{II} couple inside a 14-membered cyclic, quadridentate amine (1,4,8,11-tetraazacyclotetradecane (cyclam) and related macrocycles). Cyclam and cyclam-like ligands form stable complexes with both Ni^{II} and Ni^{III}.[6] In particular, the one-electron oxidation of the yellow low-spin $[Ni^{II}(cyclam)]^{2+}$ complex to the green low-spin trivalent complex takes place at a moderately positive potential (+ 0.73 V vs. NHE in 1 M HCl). With this background in mind, the two-component systems **3** and **4** have been synthesised, in which a nickel azacyclam subunit is linked, through a sulfonamido bridge, to the light-emitting subunit. The fluorophore in **3** is naphthalene, and in **4** the dansyl fragment (whose emission is due to a charge-transfer excited state). It will be shown that both **3** and **4** display an efficient switching activity of the same type as in systems **1** and **2** (C_{ox} quenches fluorescence; C_{red} does not). Moreover, the formally similar system **5**, in which a cyclam subunit is linked to the fluorophore (anthracene) through a $-(CH_2)-$ group has also been considered. In this case, both the forms containing Ni^{II} and the Ni^{III} quench anthracene fluorescence, so that the redox equilibrium C_{ox}–A* + $e^- \rightleftharpoons C_{red}$–A* produces the undesirable OFF/OFF situation. The efficiency of the investigated devices will be accounted for in terms of eT and ET mechanisms and related to the redox activity of the metal centres and to the structural features of the supramolecular systems. In this connection, the crystal and molecular strucure of system **4**, which has been characterised through X-ray analysis, will be described.

Results and Discussion

Synthesis of two-component systems 3 and 4: The two-component systems **3** and **4** can be synthesised through a one-pot procedure in which the Ni^{II} ion acts a template. This very convenient self-assembly process, illustrated in Figure 2 for system **3**,

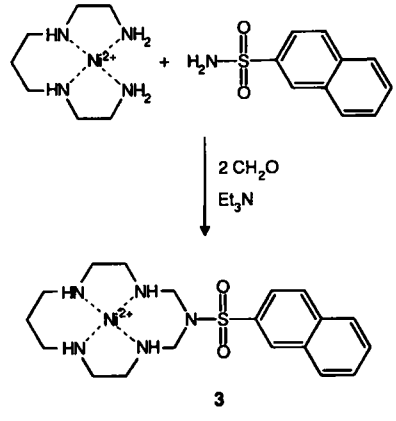

Fig. 2. The template synthesis of the two-component system **3**. System **4** is obtained through an analogous one-pot procedure, with dansylamide as the locking fragment.

involves the closure of an open-chain tetraamine, preoriented through the coordination to the metal centre, by a primary sulfonamide group, which acts as a locking fragment in presence of excess formaldehyde and base (triethylamine). According to a recently elucidated mechanism, two molecules of formaldehyde give Schiff-base condensation with the primary amine groups of the tetramine; then, the two C=N bonds undergo a nucleophilic attack by the consecutively deprotonated amide fragment.[7] The reaction is quite general, works well with any type of primary amide (carboxyamide, $RCONH_2$, or sulfonamide, RSO_2NH_2) and offers the opportunity to append any desired R functionality at a Ni^{II}–azamacrocyclic subunit.[8, 9] In the present case, the two fluorescent fragments naphthalene and *N*,*N*-dimethyl-1-aminonaphthalene could be appended to the metal-containing framework. It should be also noted that the 14-membered ring in the azacyclam acts as a tetradentate ligand in the same way as cyclam; the amide nitrogen atom plays only a structural role and is not involved at all in the coordination to the metal. Upon addition of concentrated $HClO_4$, complexes precipitated from the one-pot reaction mixture. In these yellow

0947-6539/96/0210-1244 $ 15.00+.25/0 Chem. Eur. J. 1996, 2, No. 10

perchlorate salts, the Ni^{II} cation has a low-spin electronic configuration, which results from a square-planar stereochemical arrangement. In the case of **4**, following the addition of a strongly acidic solution, a salt precipitated containing **4** protonated at the *N,N*-dimethylamino group of the dansyl fragment. Crystals of the $[4H](ClO_4)_3$ salt were suitable for an X-ray structural investigation.

Structural characterization of $[4H][ClO_4]_3$: The crystal structure contains three perchlorate anions and one cationic complex, in which the *N,N*-dimethylamino group of the ligand is protonated. A perspective view of the tripositive cationic complex is shown in Figure 3. Selected bond lengths and angles are given in Table 1.

The Ni^{II} ion is coordinated by the four secondary amine nitrogen atoms of the macrocyclic moiety, in an essentially square-planar geometry. The Ni^{II}–N bond lengths are in the range expected for the low-spin Ni^{II}–amine nitrogen bond and very similar to those observed previously in the structural investigations of low-spin Ni^{II} azacyclam derivatives.[7, 10] One perchlorate ion lies above and one below the N_4 coordination plane, and both interact through N–H···O–ClO_3^- hydrogen bonds with the secondary amines (see Table 1). In spite of two perchlorate oxygen atoms occupying the pseudoaxial positions of the metal center, the Ni^{II}···O distances [Ni···O5 = 2.93(1), Ni···O7 = 2.824(6) Å] are too long for any coordinative interaction.

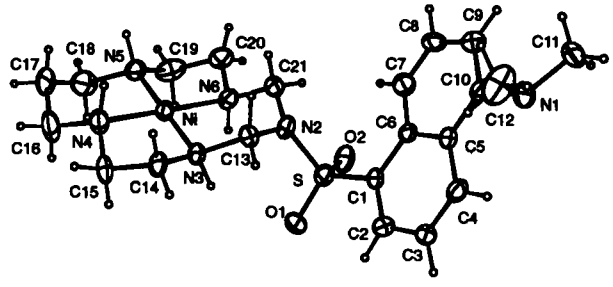

Fig. 3. Perspective view of the $[4H]^{3+}$ cation (ellipsoids at the 30% probability level).

Table 1. Crystal structure of $[4H](ClO_4)_3$.
a) Selected bond lengths (Å) and angles (°).

Ni–N3	1.945(5)	S–C1	1.767(6)	N3–C14	1.492(8)
Ni–N4	1.934(5)	N1–C10	1.477(8)	N4–C15	1.488(9)
Ni–N5	1.931(5)	N1–C11	1.507(9)	N4–C16	1.496(9)
Ni–N6	1.934(5)	N1–C12	1.50(1)	N5–C18	1.505(9)
S–O1	1.436(5)	N2–C13	1.445(8)	N5–C19	1.490(9)
S–O2	1.446(5)	N2–C21	1.444(8)	N6–C20	1.507(9)
S–N2	1.645(5)	N3–C13	1.495(7)	N6–C21	1.470(8)
N5-Ni-N6	86.1(2)	C10-N1-C11	112.9(5)	Ni-N6-C20	108.8(3)
N4-Ni-N6	177.9(2)	S-N2-C21	120.7(4)	C20-N6-C21	109.5(5)
N4-Ni-N5	94.9(2)	S-N2-C13	117.0(4)	S-C1-C6	122.3(4)
N3-Ni-N6	92.4(2)	C13-N2-C21	118.1(5)	S-C1-C2	116.4(5)
N3-Ni-N5	178.3(2)	Ni-N3-C14	109.3(3)	N2-C13-N3	111.2(5)
N3-Ni-N4	86.7(2)	Ni-N3-C13	118.4(4)	N3-C14-C15	106.3(5)
N2-S-C1	104.8(3)	C13-N3-C14	108.9(4)	N4-C15-C14	106.4(5)
O2-S-C1	110.8(3)	Ni-N4-C16	121.3(5)	N4-C16-C17	110.7(6)
O2-S-N2	104.6(3)	Ni-N4-C15	108.2(4)	C16-C17-C18	112.5(6)
O1-S-C1	106.5(3)	C15-N4-C16	109.1(5)	N5-C18-C17	111.1(7)
O1-S-N2	109.2(3)	Ni-N5-C19	108.1(4)	N5-C19-C20	105.3(6)
O1-S-O2	120.0(3)	Ni-N5-C18	118.1(4)	N6-C20-C19	105.1(6)
C11-N1-C12	110.0(6)	C18-N5-C19	111.3(6)	N2-C21-N6	111.8(5)
C10-N1-C12	111.1(5)	Ni-N6-C21	118.1(4)		

b) Relevant hydrogen bonds [a].

	D–H	H···A	D–H···A	D···A
N3(i)–H3N(i)···O6(i)	1.015(5)	2.296(6)	134.1(3)	3.089(7)
N4(i)–H4N(i)···O7(i)	1.088(6)	2.349(5)	134.8(3)	3.209(8)
N4(i)–H4N(i)···O3(ii)	1.088(6)	2.327(6)	128.6(4)	3.124(9)
N5(i)–H5N(i)···O9(i)	1.038(6)	2.484(8)	136.8(3)	3.318(9)
N6(i)–H6N(i)···O4(i)	1.026(5)	2.217(9)	148.5(4)	3.14(1)
N6(i)–H6N(i)···O8(iii)	1.026(6)	2.322(6)	110.6(2)	3.073(8)

[a] Symmetry codes: i) x, y, z; ii) $-x-1/2, y-1/2, 3/2-z$; iii) $1-x, -y, 1-z$.

The macrocyclic and sulfonamide moieties show structural features that resemble the corresponding fragment in the [3-(4-toluenesulfonyl)-1,3,5,8,12-pentaazacyclotetradecane]Ni^{II} cation:[7] the azacyclam ring has a *trans*-III configuration, with the two six-membered chelate rings in a chair conformation [apex–apex distances: Ni–N2 = 3.277(4), Ni–C17 = 3.321(7) Å] and the two five-membered rings in a twist conformation. The bis(ethylenediamine)nickel(II) fragment is in a λ–δ configuration allowed by the pseudosymmetry plane bisecting the N3-Ni-N6 and N4-Ni-N5 bond angles.

The geometrical parameters of the sulfonamido group are as expected: the N2 amide nitrogen is nearly planar, with an improper nitrogen torsion angle τ_N (S-N2-C13-C21) of −157°. Note that the angle τ_N is a sensitive index of nitrogen hybridization, as it spans from 120 (sp^3) to 180° (sp^2). The S–C1 bond is staggered with respect to the N–C bond involving the amide nitrogen (C1-S-N2-C13 = −76.1(5), C1-S-N2-C21 = 127.5(5)°).

A dihedral angle of 63.6(1)° is formed between the N_4 secondary amines plane and naphthalene plane. The analysis of the geometrical features of the *N,N*-dimethylamino group shows a clear sp^3 hybridization of the N1 nitrogen atom. In fact, 1) the improper nitrogen torsion angle τ_N (C10-N1-C11-C12) = −124.1°), 2) the significant displacement of the N1 atom from the naphthalene plane of 0.135(6) Å, and 3) the elongated N1–naphthalene distance (N1–C10 = 1.477(8) Å) are indicative for the protonation of the tertiary amine nitrogen atoms. Moreover, although it has not been possible to locate experimentally the proton in the crystal structure, the short distance between the N1 nitrogen atom and the O9 perchlorate oxygen atom is compatible with a strong hydrogen-bonding interaction: N1···O9(iv) = 2.936(8) Å (symmetry code iv: $1/2+x$, $1/2-y$, $1/2+z$).

The crystal packing is maintained by electrostatic, van der Waals and hydrogen-bonding interactions. The H-bonding network involves the four secondary amines and the tertiary protonated one, as donor atoms, and the oxygen atoms of the two perchlorate ions, axially packed with respect to the coordination plane, as acceptor atoms. The third perchlorate ion is too far from the acidic H atoms to be involved in H-bonding interactions (see crystal packing in Fig. 4).

Fluorescence redox switching through the Ni^{III}/Ni^{II} couple: The redox behaviour of **3** was investigated by means of cyclic voltammetry (CV) experiments. Figure 5 displays the CV profile obtained for an MeCN solution 2×10^{-4} M in **3** and 0.1 M in tetra-*n*-butylammonium perchlorate (Bu_4NClO_4).

The less anodic reversible wave ($E_{1/2}$ = 0.77 V vs. Fc^+/Fc; in the following discussion all the electrode potential values will be referred to the same couple) should correspond to the oxidation of the metal centre (Ni^{II}/Ni^{III}). The one-electron oxidation of Ni^{II} complexes of azacyclam macrocycles, in a 0.1 M solution of Bu_4NClO_4 in MeCN, typically falls within the 0.58–0.79 V range.[7] The more anodic irreversible wave (peak potential, E_p = 1.25 V) is ascribed to the oxidation of the naphthalene fragment of **3**. It should be noted that Ni^{III}–tetraazamacrocyclic complexes tend to assume a *trans*-octahedral stereochemistry.

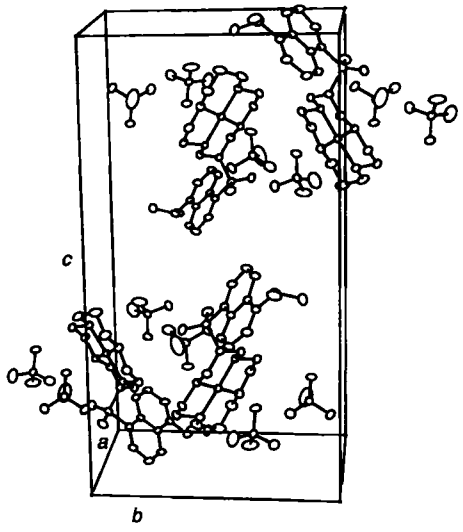

Fig. 4. Packing diagram viewed down the *a* axis. H atoms have been omitted for clarity.

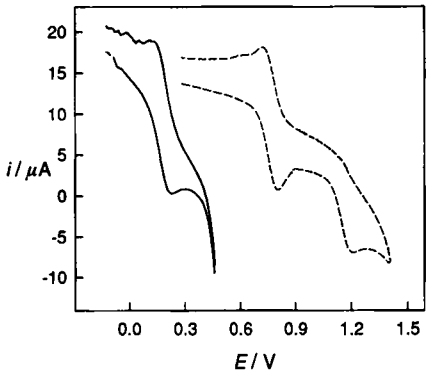

Fig. 5. Cyclic voltammograms of **3** in an MeCN solution (scan rate of 100 mVs^{-1}). 0.1 M Bu_4NClO_4 (- - -): the less anodic, reversible wave corresponds to the Ni^{II}/Ni^{III} transformation; the more anodic, irreversible wave to the oxidation of the naphthalene subunit. 0.1 M Bu_3BzNCl (—): only the wave corresponding to the Ni^{II}/Ni^{III} change is observed, prior to the anodic discharge.

In an MeCN solution, in presence of the poorly coordinating ClO_4^- ions, two solvent molecules occupy the axial positions. The Ni^{III} state can be further stabilised through axial coordination by anions with pronounced donor properties (e.g., Cl^-). In particular, in a 0.1 M solution of tri-*n*-butylbenzylammonium chloride (Bu_3BzNCl) in MeCN, the reversible oxidation of the Ni^{II} centre of the two-component system **3** took place at a much less positive potential ($E_{1/2}$ = 0.18 V) (solid line, Fig. 5). The Ni^{III} form of **3** was prepared through exhaustive electrolysis of a 0.1 M solution of Bu_3BzNCl in MeCN, by setting the potential of the working electrode (a platinum gauze) at 0.33 V. One mole of electrons per mole of **3** was consumed, and a stable green solution of the Ni^{III} derivative was obtained.

The stability of the oxidised form of **3** in solution made it possible to evaluate the effect of metal oxidation state on the emission properties of the proximate aromatic fluorophore. In particular, the Ni^{II} form of **3**, which is yellow in solution, displays the typical emission spectrum of the 2-naphthalenesulfonamide fragment (quantum yield Φ = 0.11). Exhaustive electrolysis caused this solution to lose its emission properties, with the intensity of the fluorescence spectrum being reduced to less than 2% of that observed for the Ni^{II} form (see Fig. 6). On electrolysing the solution back to the Ni^{II} form at 0.03 V, the colour turned from green to yellow and the fluorescence spectrum was

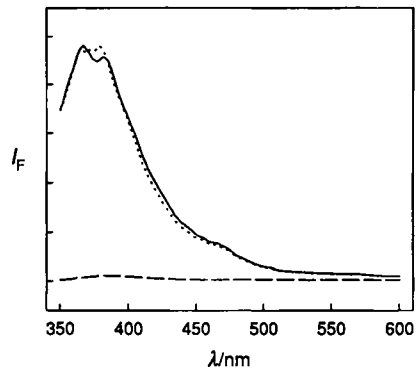

Fig. 6. Fluorescence spectra of **3** recorded during controlled-potential electrolysis: prior to electrolysis, Ni^{II} form (—); after electrolysis at 0.33 V, Ni^{III} form (– –); after electrolysis at 0.03 V, Ni^{II} form (· · ·).

fully restored (see Fig. 6). Moreover, the fluorescence of the solution could be consecutively quenched and restored through several cycles, by setting the potential of the working electrode at 0.33 and 0.03 V, without any significant signal loss.

The C–A system **3** thus displays true switching behaviour, since 1) its control unit C is fully stable in both states, and 2) only one of the two states, C_{ox}, modifies the property of the proximate active unit A. The effect is spectacular: the chosen property, fluorescence, can be consecutively extinguished and restored through a simple operation, namely, by adjusting the knob of a potentiostat.

The two-component system **4** exhibits a fluorescence switching activity analogous to that of **3**. In particular, the Ni^{II} form shows a low-energy, nonstructured emission band (Φ = 0.40), which originates from a charge-transfer excited state and is nearly coincident with the band observed for the dansylamide fragment alone.

The cyclic voltammogram, obtained for a 0.1 M solution of Bu_4NClO_4 in MeCN, showed only an irreversible wave with E_p = 0.55 V, assigned to the oxidation of the dansyl subunit. Dansylamide itself showed a similar irreversible oxidation wave with E_p = 0.47. The dansylamide fragment has a distinct tendency to undergo reduction, and it is possible that its oxidation overlaps and obscures the oxidation of the metal centre (which is expected at around 0.75–0.8 V).[7] On the other hand, in a 0.1 M Bu_3BzNCl solution, owing to the Ni^{III} stabilization effect by the Cl^- ions, the Ni^{II}/Ni^{III} transformation took place well before the oxidation of the luminescent fragment and appeared as a reversible signal in the CV profile at 0.08 V (see Fig. 7).

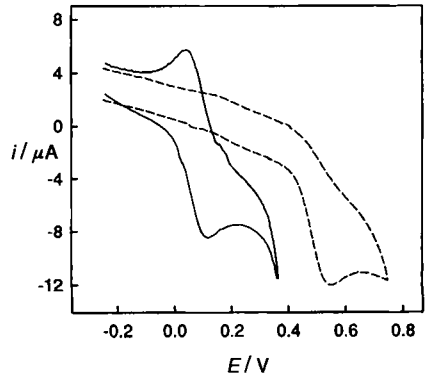

Fig. 7. Cyclic voltammograms of **4** in an MeCN solution (scan rate of 100 mVs^{-1}). 0.1 M Bu_4NClO_4 (- - -): the irreversible wave corresponds to the oxidation of the dansylamide subunit. 0.1 M Bu_3BzNCl (—): the reversible wave corresponds to the Ni^{II}/Ni^{III} transformation.

0947-6539/96/0210-1246 $ 15.00+.25/0 Chem. Eur. J. 1996, 2, No. 10

A controlled potential electrolysis experiment was carried out on an MeCN solution, 2×10^{-4} M in **4** and 0.1 M in Bu_3BzNCl, by setting the potential of the working electrode at 0.23 V. The green solution so obtained showed a much less intense fluorescence emission (less than 10% of that observed prior to the electrolysis). The working electrode potential was then set at −0.07 V: the solution turned yellow and the fluorescence was fully restored (see Fig. 8). Again, in the present system, fluores

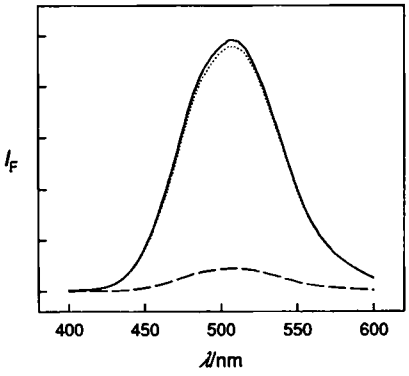

Fig. 8. Fluorescence spectra of **4** recorded during controlled-potential electrolysis: prior to electrolysis, Ni^{II} form (—); after electrolysis at 0.23 V, Ni^{III} form (– –); after electrolysis at −0.07 V, Ni^{II} form (· · ·).

cence can be switched on and off at will, by simply changing the potential of the working electrode. It should be noted that the choice of the oxidation potential is rather critical. In fact, if the potential is adjusted to 0.33 V, that is, 250 mV higher than $E_{1/2}$, fluorescence is quenched to less than 2% of the original intensity. However, in the following reductive electrolysis experiment, no more than 80% of the original fluorescence intensity is restored. This suggests that electrolysis at too high a potential also results in the partial oxidation and decomposition of the fluorescent fragment. This behaviour may be related to the fact that the oxidation of the dansylamide fragment takes place at a potential rather close to that of the oxidation of the Ni^{II} centre, much closer than that observed for the naphthalenesulfonamide subunit (system **3**).

In the third system considered, $[Ni^{II}(\mathbf{5})]^{2+}$, the Ni^{II} centre was encircled by a cyclam ring and the fluorophore was an anthracene fragment, appended to one of the amine nitrogen atoms of the tetraaza framework through a $-CH_2-$ group. The electrochemical behaviour of $[Ni^{II}(\mathbf{5})]^{2+}$ was similar to that observed for **4**: 1) the Ni^{II}/Ni^{III} transformation could not be observed by cyclic voltammetry studies in the solution containing perchlorate, probably because its CV wave was hidden by the irreversible oxidation of the anthracene fragment; 2) the reversible CV signal associated with the oxidation of the metal centre could be observed in a solution containing chloride ions (Fig. 9). However, the emission behaviour of **5** was completely different with respect to **3** and **4**. Neither the $[Ni^{II}(\mathbf{5})]^{2+}$ form nor the green solution of the Ni^{III} system, prepared through controlled potential electrolysis in a solution 0.1 M Bu_3BzNCl (working potential: 0.38 V), showed any fluorescent emission.[11] Thus, the C–A system **5** fulfils the requirement that both states be stable, but cannot work as a switch, as both its C_{red} (Ni^{II}) and C_{ox} (Ni^{III}) forms affect the signalling property of A in the same way; this produces the undesirable OFF/OFF situation.

The origin of fluorescence switching: Understanding the switching mechanism operating in systems **3** and **4** requires that the

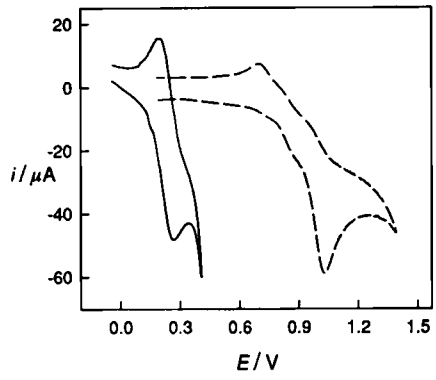

Fig. 9. Cyclic voltammograms of **5**, in an MeCN solution (scan rate of 100 mVs^{-1}). 0.1 M Bu_4NClO_4 (– –): the irreversible wave corresponds to the oxidation of the naphthalene subunit. 0.1 M Bu_3BzNCl (—): the reversible wave corresponds to the Ni^{II}/Ni^{III} transformation.

nature of fluorophore quenching by the Ni^{III} centre be elucidated, in other words, whether it is based on an eT or an ET intramolecular process. A qualitative distinction between the two mechanisms can be achieved by carrying out spectrofluorimetric studies on a frozen solution (e.g., at liquid nitrogen temperature). In the case of an intramolecular eT process, Q-to-F* or F*-to-Q (Q = quencher, F = fluorophore, in the covalently linked Q–F* system), immobilisation of the solvent molecules would raise the energy of the ion pair $Q^{\bullet+}-F^{\bullet-}$ or $Q^{\bullet-}-F^{\bullet+}$, respectively, and thus prevent the electron transfer.[12, 13] Consequently, in the presence of an eT quenching mechanism at room temperature, freezing of the solution at 77 K would fully restore the fluorescence emission. On the other hand, an ET process does not involve any charge separation and solvent reorganization, and it is expected to operate both in fluid and glassified media. Thus, freezing the solution should not cause any fluorescence revival when an ET mechanism is active.

Unfortunately, the above-mentioned procedure does not work with the systems under investigation, as the chosen solvent, acetonitrile, does not form a glass on freezing. A glass-forming medium in which all the two-component systems under investigation are soluble (and stable in their Ni^{II} and Ni^{III} forms) is ethanol. However, in contrast to the electrochemically stable MeCN, EtOH undergoes anodic discharge at a moderately positive potential and selective oxidation of the Ni^{II} centre cannot be carried achieved through controlled-potential electrolysis experiments. However, the desired oxidation could be performed chemically, by using peroxydisulfate as an oxidising agent, in a 95/5 $EtOH/H_2O$ solution, adjusted to 0.1 M ionic strength with NaCl. In fact, on addition of $S_2O_8^{2-}$ to an aqueous ethanolic solution of both **3** and **4**, the green colour of the Ni^{III} form appears. The process is reversible, as the yellow colour of the Ni^{II} system is quickly restored on addition of the reducing agent NO_2^-. This redox process can be repeated for several cycles, provided that only a moderate excess of the oxidising and reducing agent is added each time. As far as the spectrofluorimetric studies at 77 K are concerned, the following behaviour was observed: 1) freezing of the solutions of the Ni^{III}-containing systems **3** and **4** caused a full restoration of the emission spectrum (quenching mechanism: eT); 2) no fluorescence revival was observed for both the Ni^{II} and Ni^{III} forms of **5** (quenching mechanism: ET).

Thus, it appears that the desirable ON/OFF switching observed with systems **3** and **4** results from the fact that an eT quenching mechanism operates in presence of the Ni^{III} centre and not in

presence of Ni^{II}. The two eT processes can be described by the Equations (1) and (2). The value of the free energy change

$$Ni^{III} + F^* \longrightarrow Ni^{II} + F^{\cdot +} \quad (1)$$

$$Ni^{II} + F^* \longrightarrow Ni^{III} + F^{\cdot -} \quad (2)$$

associated with each eT process, ΔG°_{eT}, can be estimated through the combination of the relevant photophysical and electrochemical parameters [Eqs. (3) and (4)]. E^*_F represents the energy gained by the fluorophore on photoexcitation, which can be calculated from the energy of the emission band, and E° is the standard electrode potential, which can be approximated to the $E_{1/2}$ value obtained through voltammetric studies. Whereas the $E_{1/2}$ values for couples involving the metal centres are quite reliable in view of their full electrochemical reversibility, the corresponding quantities relating to the F subunit are taken from poorly reversible or irreversible voltammetric waves and should be considered with care. The $\Delta G^\circ_{eT}(1)$ and $\Delta G^\circ_{eT}(2)$ values for systems **3** and **4** are given in Table 2.

$$\Delta G^\circ_{eT}(1) = -E^*_F - eE^\circ(Ni^{III}/Ni^{II}) + eE^\circ(F^+/F) \quad (3)$$

$$\Delta G^\circ_{eT}(2) = -E^*_F + eE^\circ(Ni^{III}/Ni^{II}) - eE^\circ(F/F^-) \quad (4)$$

Table 2. Electrochemical and photophysical quantities used to calculate ΔG°_{eT} in two-component systems **3** and **4**.

	3	**4**
$E^\circ(Ni^{III}/Ni^{II})$/V [a,b]	0.18	0.08
$E^\circ(F^+/F)$/V [a,c]	1.21	0.55
$E^\circ(F/F^-)$/V [a,c]	−2.9	≤ −3.0 [d]
E^*/eV	3.3	2.4
$\Delta G^\circ_{eT}(Ni^{II}$-to-$F^*)$/eV	−0.2	≥0.7
$\Delta G^\circ_{eT}(F^*$-to-$Ni^{III})$/eV	−2.3	−1.9

[a] V vs. Fc^+/Fc, in MeCN solution at 25 °C (Fc = ferrocene). [b] $E_{1/2}$ values in 0.1 M Bu_3BzNCl. [c] Irreversible peak, E_p, in 0.1 M Bu_4NClO_4. [d] No peaks were observed in the cathodic scan until −3.0 V.

The data reported in Table 2 give a qualitative thermodynamic account for the switching behaviour of **3** and **4**. In fact, for both systems the F^*-to-Ni^{III} eT process (responsible for switching off the fluorescence) is characterised by a very negative $\Delta G^\circ_{eT}(1)$ value. In contrast, the Ni^{II}-to-F^* eT process is much less favoured, with a positive or slightly negative $\Delta G^\circ_{eT}(2)$ value. The fluorescence redox switching behaviour of system **3** is illustrated pictorially in Figure 10.

In the other system considered, **5**, an ET quenching mechanism operates with both the Ni^{II} and Ni^{III} forms (OFF/OFF behaviour). Ni^{II} (electronic configuration: d^8) and Ni^{III} (d^7) ions, like all transition-metal ions, provide an empty or half-filled d level of suitable energy to be involved in a double electron exchange process, which leads to an ET mechanism of the Dexter type. In particular, the metal-containing component, both in the Ni^{II} and Ni^{III} state, displays absorption bands that overlap, at least partially, with the emission band of the anthracene fragment. It should be also noted that the eT mechanism, if active in system **5**, would also generate the OFF/OFF situation. In fact, both $\Delta G^\circ_{eT}(1)$ and $\Delta G^\circ_{eT}(2)$ are distinctly negative (− 2.5 and −1.1 eV, respectively).

The fact that systems **3** and **4** operate through an eT mechanism and **5** through an ET mechanism may depend on other factors besides redox tendencies and electronic configurations

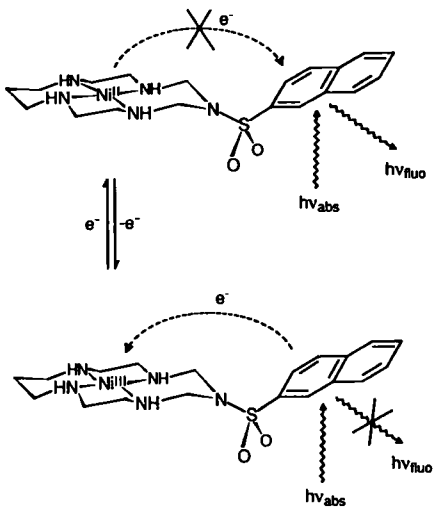

Fig. 10. The mechanism of the redox switching of fluorescence in the two-component system **3**: the oxidised form induces a fluorophore-to-Ni^{III} electron transfer process, which quenches fluorescence; the reduced form does not. A similar mechanism operates in system **4**.

of the metal ions of the control subunit. Firstly, the distance between the metal and the fluorophore can play a significant role. In particular, molecular mechanics modelling has shown that the distance between the metal centre and the closest carbon atom of the fluorescent subunit (i.e., that connected to the spacer) is rather small for system **5** (4.1 Å). The distance obtained from the crystal structure of system **4** is distinctly larger (Ni−C1 = 5.87 Å; this compares well with the distance calculated by molecular mechanics: 5.9 Å; a similar distance can be estimated for system **3**). It has been demonstrated that the rates of ET processes decrease with increasing spacer length much faster than those of the corresponding eT processes.[14] Thus, at a longer distances, the eT mechanism is expected to prevail over the ET mechanism. Moreover, the nature of the spacer connecting the control subunit and the fluorescent fragment may also have some effect. In this connection, we note that system **5** is rather flexible, and the $-CH_2-$ spacer may allow folding and occasional intramolecular van der Waals contact between the metal-containing subunit and the anthracene fragment, which may favour the ET process. The more rigid sulfonamide spacers of systems **3** and **4** prevent folding and do not permit a close contact of the two components. Moreover, rigidity and extended π bonding over the $-SO_2N<$ bridging group may favour intramolecular through-bond electron transfer. Such a mechanism has been shown to operate in rigid systems at a distance as large as 20 Å.[15] More specific examples are required to support the existence of a relationship between the mechanism of signal transduction and the nature of the spacer in two-component fluorescence switches. Notably, the previously reported metal-centred redox switch, **2**,[5] is another example in which an eT mechanism is observed in a species containing a rigid spacer (an ester group). The distance between the metal centre (a $[Cu^{II,I}(thiacyclam)]^{2+/+}$ complex) and the C9 atom of the anthracene subunit is especially long in **2** (7.1 Å, calculated by molecular modelling).

Conclusions

This work has demonstrated that the design of fluorescence switching systems of a supramolecular nature can substantially profit from transition metals. In fact, transition metals typically

0947-6539/96/0210-1248 $ 15.00+.25/0 Chem. Eur. J. 1996, 2, No. 10

present different oxidation states of varying stability and offer the best opportunity to create bistable systems. For a given metal, an appropriate ligand can be found capable of stabilising two adjacent oxidation states to a comparable extent. This is the case for tetraaza macrocycles (e.g., cyclam and azacyclam) with the $Ni^{III,II}$ couple and for tetrathia macrocycles (e.g., thiacyclam) with the $Cu^{II,I}$ couple. Fluorescence switching activity requires that only one of the two oxidation states quenches the proximate photoexcited fluorophore, and this can be understood (and programmed) on a thermodynamic basis provided that the quenching process rests on an eT mechanism. In particular, we observed that the higher oxidation state of the bistable couple (Ni^{III} and Cu^{II}) induces the eT process and the lower one (Ni^{II} and Cu^{I}) does not. For the systems considered, all of which contain an aromatic light-emitting fragment (naphthalene, anthracene), the above behaviour is to be ascribed ultimately to the fact that the oxidation of the fluorophore (F-to-F^+) is a much easier process than its reduction (F-to-F^-). Transition metals could be also used for designing fluorescence switches operating through an ET mechanism (a goal which has not yet been achieved). As an example, a couple composed of ions having a d^{10} and a d^9 electronic configuration (e.g., Cu^{I} and Cu^{II}) could work well, as only the d^9 cation can be involved in the double electron exchange mechanism and would quench the fluorophore. System **2** is based on a Cu^{I}/Cu^{II} couple, but it "prefers" to operate through the eT mechanism. Thus, the main problem yet to be solved is the elucidation of the structural factors that determine the nature of the signal transduction mechanism—eT or ET—in the covalently linked C–A system. It is probable that such factors are related to the properties of the spacer linking C and A components, such as, degree of flexibility, electron permeability and length.

Experimental Procedure

Materials: Unless otherwise stated, commercial-grade chemicals were used without further purification.

N,N'-Bis(2-aminoethyl)propane-1,3-diamine (2·3·2-tet) was prepared as described for the analogous tetramine 3·2·3-tet [16], distilled at reduced pressure (125 °C; 5×10^{-2} Torr) and stored over NaOH in the refrigerator. 1-(Anthracen-9-ylmethyl)-1,4,8,11-tetraazacyclotetradecane (**5**) was prepared as previously described [17].

Crystal structure determination: Crystals suitable to X-rays diffraction study were obtained from slow crystallization from an EtOH/water solution of $[\mathbf{4}]Cl_2$, to which 65% aqueous $HClO_4$ had been added. Unit cell parameters and intensity data were obtained on Enraf-Nonius CAD-4 diffractometer at Centro Grandi Strumenti, Università di Pavia. Calculations were performed with the MolEN software on a MicroVax-3100 computer [18]. Crystal data and the most relevant parameters used in the crystallographic study are reported in Table 3. The cell dimensions were determined by least-squares fitting of 25 centered reflections monitored in the range $27 < \theta < 37°$. Correction for Lp and empirical absorption were applied [19]. The structure was solved by Patterson function. The non-hydrogen atoms were refined anisotropically by full-matrix least-squares. The hydrogen atoms of the four secondary amines were found in the difference Fourier map while the positions of the others were calculated at convergence by program HYDRO [19]. The H atom on the protonated dimethylamino group, not found in the Fourier map, was disregarded. All the H atoms were inserted with an isotropic displacement factor proportional (×1.3) to those of their neighbouring atoms and not refined. Perchlorate oxygen atoms O5, O11, O12 and O13 are disordered: alternative positions were observed, inserted in the model and refined anisotropically. Relative occupancies: O5:O5' 0.7:0.3, O11:O11' 0.7:0.3, O12:O12' 0.65:0.35, O13:O13' 0.70:0.30. Atomic scattering factors were taken from literature [20]. Diagrams of the molecular structure were performed by ORTEP program [21].

Crystallographic data (excluding structure factors) for the structure reported in this paper have been deposited with the Cambridge Crystallographic Data Centre as supplementary publication no. CCDC-1220-20. Copies of the data can be obtained free of charge on application to The Director, CCDC, 12 Union Road, Cambridge CB2 1EZ, UK (Fax: Int. code + (1223)336-033; e-mail: teched@chemcrys.cam.ac.uk).

Table 3. Crystal and refinement data for $[\mathbf{4H}](ClO_4)_3$.

formula	$C_{21}H_{35}N_6O_{14}SCl_3Ni^{II}$
M_r	792.67
crystal colour	pale orange
crystal size	0.25 × 0.14 × 0.14
system	monoclinic
space group	$P2_1/n$
a/Å	8.523(1)
b/Å	14.319(1)
c/Å	25.801(3)
α, β, γ/°	90, 98.00(1), 90
V	3118.1(5)
Z	4
ρ_{calcd}/Mg m^{-3}	1.689
radiation	$Cu_{K\alpha}$ (λ = 1.54184 Å) graphite monochromated
μ/mm^{-1}	4.601
T/K	293(3)
θ/°	2–70
scan type	$\omega - 2\theta$
reflns measured	$-10 < h < 10$; $0 < k < 17$; $-8 < l < 31$
transmission coeff.	T_{min} 0.876; T_{max} 0.998
standard reflections	3 every 300 reflns
max. decay/%	− 0.5
tot. reflns measured	8593
unique reflections	4931
R_{int}	0.024
obs. reflns [$I > \sigma(I)$]	4371
refinement type	F
R [a]	0.085
G. O. F.	1.390
R_w [$w = 1/\sigma(F)^2$] [b]	0.077
refined parameters	451
$(\text{shift/e.s.d.})_{max}$	0.2
final fourier map/e Å^{-3}	max 0.618, min −0.216
scale factor	0.960

[a] $R = \sum||F_o| - |F_c||/\sum|F_o|$. [b] $Rw = [\sum w(|F_o| - |F_c|)^2/\sum w(F_o)^2]^{1/2}$.

Electrochemical experiments: MeCN was distilled over CaH_2 and stored under nitrogen over molecular sieves. $[Bu_4N]ClO_4$ and $[Bu_4BzN]Cl$ (Fluka) were used as supporting electrolytes. Electrochemical measurements (cyclic voltammetry, CV, and differential pulse voltammetry, DPV) were performed in a conventional three-electrode cell, using a P. A. R. 273 potentiostat/galvanostat, under control of a personal computer. The working electrode was a platinum microsphere and the counter-electrode was a platinum foil. A silver wire was used as a pseudoreference electrode and was calibrated using ferrocene as an internal standard. Thus, all the potentials reported in this work have been referenced to the classical Fc^+/Fc (Fc = ferrocene) standard couple. Controlled potential coulometry experiments were performed on solutions $2-5 \times 10^{-4}$ M in the two-component system, using a platinum gauze as a working electrode. The counter-electrode compartment was separated by the working compartment by a U-shaped bridge, filled by an MeCN solution 0.1 M in $[Bu_4BzN]Cl$.

Other physical measurements: UV/Vis spectra were measured on a Hewlett-Packard 8452A diode array spectrophotometer. Emission spectra were taken on a Perkin-Elmer LS-50 luminescence spectrometer and were corrected for instrumental response by using quinine sulfate as fluorescent standard. The relative quantum yields of fluorescence in ethanol were obtained through the optically dilution method [22]. Naphtalene (Φ = 0.21 in EtOH) [23] and 1-(dimethylamino)-5-naphthalenesulfonamide (dansylamide, Φ = 0.39 in EtOH) [24] were used as references for systems **3** and **4**, respectively. Emission spectra at 77 K were measured by using quartz sample tubes and the same luminescence spectrometer equipped with a low-temperature luminescence accessory (Perkin-Elmer).

[3-(Naphthalene-2-sulfonyl)-1,3,5,8,12-pentaazaciclotetradecane]nickel(II) chloride ($[\mathbf{3}]Cl_2$): A solution of 2·3·2-tet (0.21 g, 1.3 mmol) in ethanol (25 mL) was slowly added to a solution of $NiCl_2 \cdot 6H_2O$ (0.31 g, 1.3 mmol) in ethanol (20 mL) under magnetic stirring. The violet complex solution was warmed to 50 °C, and 2-naphthalenesulfonamide (0.27 g, 0.13 mmol), triethylamine (0.2 mL) and 35% aqueous formaldehyde (1 mL) were added. Heating and stirring were maintained for a period of a week, during which a violet precipitate formed. This was filtered through a sintered glass funnel, washed with cold ethanol and dried in vacuo. Yield 62%. $C_{19}H_{29}Cl_2N_5NiO_2S$ (521.13): calcd C 43.79, H 5.61, N 13.44; found C 43.44, H 5.50, N 13.54.

{Dimethyl[5-(1,3,5,8,12-pentaazaciclotetradecane-3-sulfonyl)naphthalen-1-yl]-amine}nickel(II) chloride ($[\mathbf{4}]Cl_2$): The complex was prepared by following the same experimental procedure described for $[\mathbf{3}]Cl_2$, but using 5-dimethylamino-

1-naphthalenesulfonamide (dansylamide) as locking fragment. Yield 48%. $C_{21}H_{34}Cl_2N_6NiO_2S$ (562.1): calcd C 44.87, H 5.74, N 14.95; found C 44.33, H 5.63, N 15.24.

[1-(Anthracen-9-ylmethyl)1,4,8,11-tetraazacyclotetradecane]nickel(II) perchlorate ([**5**]$(ClO_4)_2$): An aqueous solution of $Ni(ClO_4)_2$ (1.7 mL, 0.294 mol L^{-1}) was added portionwise to a boiling ethanol solution of **5** (0.2 g, 0.51 mmol in 50 mL). The mixture refluxed for 20 min and then allowed to cool to room temperature. An orange microcrystalline solid precipitated. This was filtered through a sintered glass funnel, washed with water and dried in vacuo. Yield 91%. $C_{25}H_{34}Cl_2N_4NiO_8$ (648.16): calcd C 46.33, H 5.29, N 8.64; found C 46.09, H 5.05, N 8.34.

Acknowledgements: This work was supported by the Italian National Council of Researches (CNR—Progetto Strategico "Tecnologie Chimiche Innovative"). A. H. V. is grateful to the ERASMUS Bureau of the European Union for an ECTS grant.

Received: February 27, 1996 [F309]

[1] J.-M. Lehn, *Supramolecular Chemistry*, VCH, Weinheim **1995**, p. 90.
[2] L. Fabbrizzi , A. Poggi, *Chem. Soc. Rev.* **1995**, 197–202.
[3] V. Balzani, F. Scandola, *Supramolecular Photochemistry*, Ellis Horwood, London, **1991**, p. 73.
[4] V. Goulle, A. Harriman, J.-M. Lehn, *J. Chem. Soc. Chem. Commun.* **1993**, 1034.
[5] G. De Santis, L. Fabbrizzi, M. Licchelli, C. Mangano, D. Sacchi, *Inorg. Chem.* **1995**, *34*, 3581.
[6] L. Fabbrizzi, *Comments Inorg. Chem.* **1985**, *4*, 33.
[7] F. Abbà, G. De Santis, L. Fabbrizzi, M. Licchelli, A. M. Manotti Lanfredi, P. Pallavicini, A. Poggi, and F. Ugozzoli, *Inorg. Chem.* **1994**, *33*, 1366.
[8] A. De Blas, G. De Santis, L. Fabbrizzi, M. Licchelli, A. M. Manotti Lanfredi, P. Pallavicini, A. Poggi, F. Ugozzoli, *Inorg. Chem.* **1993**, *32*, 106.
[9] G. De Santis, L. Fabbrizzi, M. Licchelli, C. Mangano, P. Pallavicini, *Inorg. Chem.* **1993**, *32*, 3385.
[10] L. Fabbrizzi, A. M. Manotti Lanfredi, P. Pallavicini, A. Perotti, A. Taglietti, F. Ugozzoli, *J. Chem. Soc. Dalton Trans.* **1991**, 3263
[11] The metal-free system **5**, in an MeCN solution, also does not show any fluorescent emission. However, the typically structured emission spectrum of the anthracene fragment can be observed if the solution of the metal-free system is acidified with conc. HCl. In fact, in absence of metal ions or protons, the tertiary nitrogen atom in system **5** quenches the proximate photoexcited anthracene fragment An* through an N-to-An* eT process. On protonation, the electron pair of the tertiary amine group is no longer available for eT and fluorescence is restored.
[12] M. R. Wasielewski, G. L. Gaines III, M. P. O'Neil, M. P. Niemczyk, W. A. Svec in *Supramolecular Chemistry* (Eds.: V. Balzani, L. De Cola), Kluwer Academic Publishers, Dordrecht, **1992**, p. 202.
[13] J.-P. Sauvage, J.-P. Collin, J.-C. Chambron, S. Guillerez, C. Coudret, V. Balzani, F. Barigelletti, L. De Cola, L. Flamigni, *Chem. Rev.* **1994**, *94*, 993.
[14] G. L. Closs, M. D. Johnson, J. R. Miller, P. Piotrowiak, *J. Am. Chem. Soc.* **1989**, *111*, 3751.
[15] J. R. Bolton, T. F. Ho, S. Liauw, A. Siemiarczuk, C. S. K. Wan, A. Weedon, *J. Chem. Soc. Chem. Commun.* **1984**, 559.
[16] E. K. Barefield, F. Wagner, A. W. Herlinger, A. R. Dahl, *Inorg. Synth.* **1975**, *16*, 220.
[17] L. Fabbrizzi, M. Licchelli, P. Pallavicini, A. Perotti, A. Taglietti, D. Sacchi, *Chem. Eur. J.* **1996**, *2*, 75–82.
[18] *MolEN, An Interactive Structure Solution Procedure*, Enraf-Nonius, Delf, The Netherlands, **1990**.
[19] A. C. T. North, D. C. Phillips, F. S. Mathews, *Acta Crystallogr.* **1968**, *A24*, 351.
[20] *International Tables for X-ray Crystallography*, Kynochn Birmingham, England, Vol. 4, **1974**, pp. 99–101 and 149–150.
[21] C. K. Johnson, *ORTEP, Report ORNL-3794*, Oak Ridge National Laboratory, Oak Ridge TN, USA, **1976**.
[22] J. N. Demas, G. A. Crosby, *J. Phys. Chem*, **1971**, *75*, 991.
[23] J. Malkin, *Photophysical and Photochemical Properties of Aromatic Compounds*, CRC Press, Boca Raton FL, USA, **1992**.
[24] Y.-H. Li, L.-M. Chan, L. Tyer, R. T. Moody, C. H. Himel, D. M. Hercules, **1975**, *97*, 3118.